Desalination and Water Treatment
www.deswater.com

doi: 10.5004/dwt.2021.27845

242 (2021) 128–143
December

Preparation and evaluation of epoxy resins for the selective removal of Cs^+ in high-level liquid waste

E.C. Escobar[a,b], R.E.C. Torrejos[a,c], J.E.L. Sio[a], H. Kim[a], W.-J. Chung[a,*], G.M. Nisola[a,*]

[a]*Environmental Waste Recycle Institute (EWRI), Department of Energy Science and Technology (DEST), Myongji University, Myongji-ro 116, Cheoin-gu, Yongin-si, Gyeonggi-do, South Korea 17058, Tel. +82-31-330-6687; Fax: +82-31-337-2902; emails: wjc0828@gmail.com (W.-J. Chung), grace.nisola@gmail.com (G.M. Nisola), ecescobar121212@gmail.com (E.C. Escobar), reytorrejos@gmail.com (R.E.C. Torrejos), edward.sio990@gmail.com (J.E.L. Sio), hernkim@mju.ac.kr (H. Kim)*

[b]*Department of Engineering Science, College of Engineering and Agro-Industrial Technology, University of the Philippines Los Baños, College Laguna, Philippines*

[b]*Department of Science and Technology-Central Office (DOST-CO), Philippine Textile Research Institute (PTRI), Taguig, Metro Manila, Philippines*

Received 21 May 2021; Accepted 24 September 2021

ABSTRACT

Selective Cs^+ sequestration from nuclear water waste is an important pre-concentration step prior to long-term storage. However, material development had so far been limited to calixarene-based sorbents. Herein, new types of epoxy resins were prepared and screened for Cs^+ capture in highly acidic (3 M HNO_3) simulated high-level liquid waste (HLLW). The resins were synthesized using bis-epoxides as the major binding component for Cs^+ and diamines as curing agents. The effects of different bis-epoxides and diamines on the selectivity and capacity for Cs^+ were identified and explained. Results reveal that the most Cs^+-selective resin is prepared from a bis-epoxide whose oxygen and sulfur donor atoms are in ortho position to a central benzene moiety that is cured with diaminopropane (resin BE2-Ep). BE2-Ep is a yellow glassy resin that is thermally stable and mechanically tough in an acidic medium. It registers a maximum capacity of 1.004 mmol g^{-1} (133.5 mg g^{-1}) which is higher than that of known Cs^+ sorbents used in highly acidic media. BE2-Ep is most selective towards Cs^+, rejecting other competing metal ions in simulated HLLW. BE2-Ep is one of the very few Cs^+-selective sorbents that can be applied in HLLW for the long-term storage of radioactive wastes.

Keywords: Adsorption; Cesium removal; Cross-linked sorbent; Epoxy resin; High-level liquid waste; Selective sequestration

---

1. Introduction

The nuclear power industry which supplies 10% of the world's electricity has continued to grow despite concerns about radioactive material release to the environment [1–3]. Management of radioactive or high-level liquid wastes (HLLW) containing Cs^{137}, a fission product generated in great quantities, remains a big challenge. Cs^{137} has a half-life ~ 30 y and decays via beta and gamma-ray emissions. Thus, the most common treatment for HLLW with Cs^+ is through natural decay to reduce its radioactivity to background levels [4,5]. Moreover, because of the high environmental mobility of Cs^+, it must be confined in customized vessels to prevent its accidental release [6,7]. Practical considerations dictate that Cs^+ must be concentrated in suitable adsorbents prior to long-term storage [8].

The sequestration of Cs^+ via adsorption had been the focus of many studies since it complements the waste solidification step before the concentrated radioactive waste is stored [4]. However, most studies have dealt with the treatment of contaminated surface waters and very few have reported on adsorptive Cs^+ sequestration from HLLW.

---

[*] Corresponding authors.

HLLW contains a variety of interfering metal ions which undermines selective sequestration of Cs^+ and contains high concentrations of oxidizing acid (~3 M HNO_3) which adversely affects the sequestration capacity of adsorbents.

Prussian blue [9,10], zeolites [5,11], layered metal sulfides [12,13] and Cs^+-imprinted polymers [14–16] have so far been employed as sorbents at mildly acidic to near neutral pH conditions since these materials either deteriorate or lose their performance in strong acid. Very few have been employed to treat acidic HLLW, and so far these sorbents have been prepared only with calixarenes or its derivatives via impregnation in macroporous silica [7,17,18] or polymeric resin [19,20] or grafting onto mesoporous carbon [21]. Unfortunately, sorbents prepared via impregnation of calixarenes in supports register low adsorption capacities (0.21 mmol g^{-1}) and exhibit ligand loss. Meanwhile, the capacity of grafted calixarenes on support is limited by its loading [20]. So far, the most promising sorbent is calix[4]arene-crown-6 grafted on mesoporous carbon with an adsorption capacity of 0.96 mmol g^{-1} at 3 M HNO_3 [21]. Thus, if the requirement for support is eliminated, higher adsorption capacities can be achieved. Moreover, considering the low availability, high cost and difficult synthesis of calixarenes, the development of other sorbents which do not require solid supports could address these limitations.

Amine-cured epoxides produce chemically-resistant crosslinked macromolecules as resins [22], allowing them to withstand highly acidic conditions. These materials possess excellent properties making them useful in many engineering applications [23,24]. Meanwhile, their preparation and use as adsorbents had rarely been studied. Unlike most organic sorbents intended for HLLW, polymeric epoxy resins do not require immobilization onto solid supports, thus, high sorption capacities may be achieved. Also, epoxy resins are dense solids that separate easily from the bulk liquid phase, eliminating the need for elaborate sorbent recovery steps prior to storage.

In this study, a new class of sorbents for the sequestration of Cs^+ in HLLW is presented. Three types of low molecular weight oxygen- and sulfur-bearing bis-epoxides (BE) as binding sites for Cs^+ were reacted with aliphatic diamine curing agents to obtain highly crosslinked epoxy resins as Cs^+ adsorbents. The effects of diamine linker length, BE structure, and complexing atom were correlated with their adsorption performance particularly in terms of their capacity and selectivity for Cs^+ in simulated HLLW. Finally, the adsorption behavior of the most Cs^+-selective epoxy resin was evaluated. This is the first report on epoxy resins with innate selectivity and capacity for Cs^+ in highly acidic HLLW.

2. Experimental

2.1. Materials

Commercially available bis-epoxide (BE) 1,4-cyclohexanedimethanol diglycidyl ether (technical grade) was purchased from Sigma-Aldrich (MO, USA) whereas BEs 1,2-bis(oxiran-2-ylmethoxy)benzene] and 2-(((2-(oxiran-2-ylmethoxy)phenyl)thio)methyl)oxirane were synthesized according to previous reports [25,26] described in the Supplementary Information. Ethylenediamine (99+ %, extra pure), catechol (99+ %), and thiourea (99+ %) were manufactured by Acros Organics (USA) while 1,3-diaminopropane (98%) and epichlorohydrin (99%) were produced by Alfa Aesar (Germany). Dimethyl sulfoxide (99.9% DMSO) was manufactured by Fisher Scientific (UK). Methanol (99.5% MeOH) and hydrochloric acid (>36% RHM grade HCl) were purchased from Samchun Chemical Co., Ltd., (Korea). Nitric acid (70% RHM grade HNO_3) was manufactured by DaeJung Chemicals and Metals (Korea). High purity metal chloride salts (CsCl, $SrCl_2$, NaCl, $BaCl_2·2H_2O$) were purchased from Alfa Aesar (Korea). High purity metal salts RbCl and $Cr(NO_3)_3·9H_2O$ were purchased from Sigma-Aldrich (MO, USA) while $Ni(NO_3)_2·6H_2O$ was purchased from DaeJung Chemicals and Metals (Korea). Deionized (DI) water (18.2 mΩ cm^{-1} at 25°C) was processed through a Millipore Milli-Q system.

2.2. Synthesis and processing of amine-cured epoxy resin sorbents

Epoxy resins were prepared using different BEs and diamines. For convenience, the BEs were labeled as follows: BE1 for [1,2-bis(oxiran-2-ylmethoxy)benzene], BE2 for [2-(((2-(oxiran-2-ylmethoxy)phenyl)thio)methyl)oxirane], and BE3 for [1,4-cyclohexanedimethanol diglycidyl ether] (Fig. 1a).

The amount of solvent (DMSO) relative to the amount of BE influenced the solidity of the final product. For this reason, initial tuning of the BE to solvent (BE*n*/DMSO) weight ratio was performed to obtain solid resins which are amenable to subsequent size reduction procedures (Table S1). The curing procedure was performed by transferring the desired amount of BE, diamine and DMSO in a glass tube (Fig. 1b). The vessel was sealed and the materials were vortex-mixed for 2 min, and then sonicated for another 2 min. The vessel was transferred to an oil bath set at 80°C where the materials were allowed to react for 1 h. Thereafter, the temperature was raised to 150°C and maintained for 4 h to complete the curing process. Solid resins were crushed and washed multiple times with methanol to remove excess reagents and solvent, and then dried under vacuum at 60°C for 12 h. Dried resins were further ground, sieved (500 μm), and then washed in 2 M HCl for 24 h at 300 rpm to remove pre-adsorbed metal ions. Thereafter, the granules were washed thoroughly with DI water until the washing registered a neutral pH, and then washed further with acetone. Final epoxy resin adsorbents were obtained after vacuum drying at 60°C for 12 h.

2.3. Sorbent evaluation and screening

The epoxy resins were screened for their adsorption performance both in terms of capacity and selectivity using simulated HLLW from spent nuclear fuel processing containing Na^+ (66.04 mM), Cr^{3+} (4.96 mM), Ni^{2+} (4.52 mM), Rb^+ (5.01 mM), Sr^{2+} (8.50 mM), Cs^+ (19.50) and Ba^{2+} (11.89 mM) in 3 M HNO_3 [27]. The adsorption process involved adding a measured amount of resin (m) in simulated HLLW with known volume (V) at a solid to liquid (S/L) ratio of 0.5 (mg mL^{-1}). The samples were mixed at 300 rpm and equilibrated for 12 h at 30°C. Thereafter, aliquots of liquid samples were obtained and passed through a 0.2 μm syringe filter,

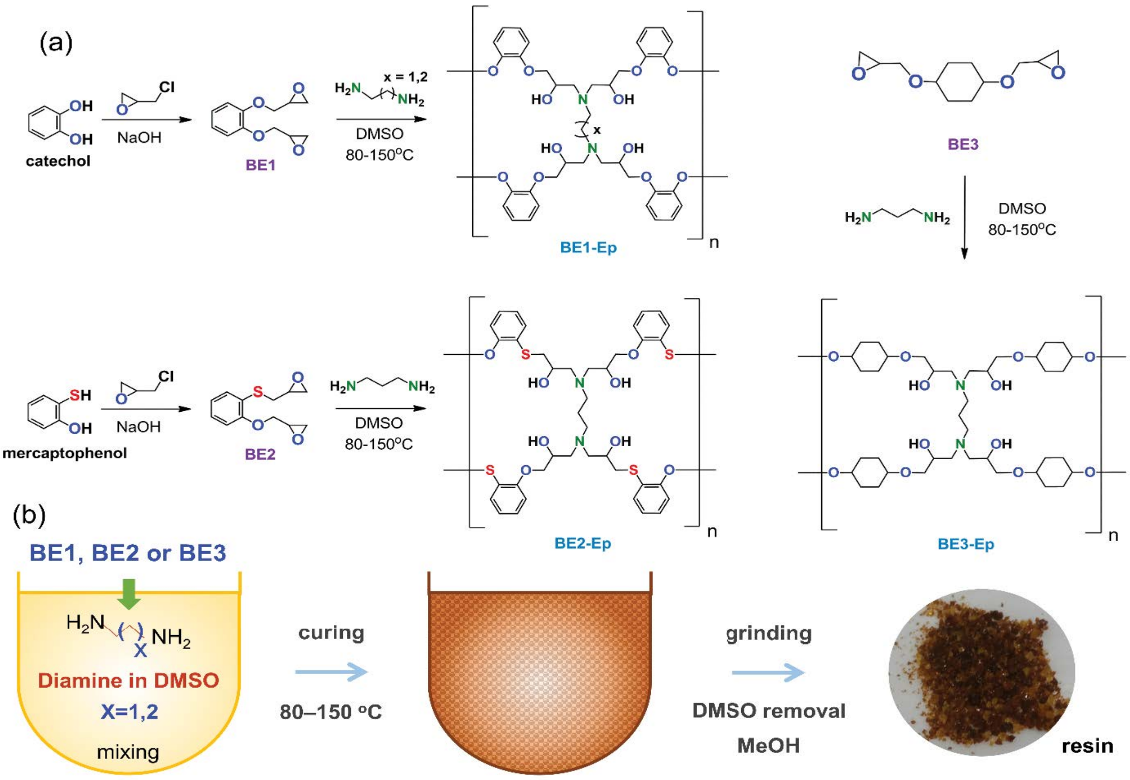

Fig. 1. (a) Bis-epoxides used as main binding sites for Cs^+ and (b) general procedure for the synthesis of crude epoxy resins.

and then acid-digested using a microwave oven (MARS-5 CEM, USA). The concentrations of metal ions in the feed (C_0) and after adsorption runs (C_e) were determined by inductively coupled plasma mass spectroscopy (ICP-MS Agilent 7500 series, USA). The adsorption capacity (Q) for each metal ion was calculated using Eq. (1) whereas the distribution coefficients (K_D) were estimated using Eq. (2). The selectivity (α) of the resin towards Cs^+ versus other metal ions was determined using Eq. (3).

$$Q = \frac{\left(C_0 - C_e\right)V}{m} \tag{1}$$

$$K_D = \frac{Q}{C_e} \tag{2}$$

$$\alpha_{Cs^+/M^{n+}} = \frac{Q_e / C_e\left(Cs^+\right)}{Q_e / C_e\left(M^{n+}\right)} \tag{3}$$

The effect of diamine curing agent was investigated in BE1 wherein the Q and α of the resin cured with ethylenediamine (BE1-Ep-Et) were compared with that cured with diaminopropane (BE1-Ep-Pr). Meanwhile, the effect of BE reactive arm opening was observed by comparing the Q and α of resins containing BE1 and BE3. Lastly, the effect of coordinating donor atoms was examined by comparing the performance of resins containing BE1 and BE2.

2.4. Adsorption experiments

The most Cs^+-selective epoxy resin (BE2-Ep) was subjected to further experiments to determine its Cs^+-adsorption isotherm, kinetic, and thermodynamic behaviors. Equilibrium isotherm runs were carried out using different initial Cs^+ concentrations (65–1,340 mg L^{-1}) in 3 M HNO_3 for 12 h to obtain its maximum adsorption capacity (Q_{max}). Adsorption time profile using BE2-Ep was also acquired at C_0 = 570 mg L^{-1} in 3 M HNO_3 to determine the kinetics of Cs^+ adsorption. For samples in the kinetic study, aliquots from batch adsorption setups were collected individually to determine the Cs^+ concentration (C_t) and capacity (Q_t) at a certain adsorption time (t) using Eq. (4). Experiments for the thermodynamics of adsorption were performed using C_0 = 1330 mg L^{-1} Cs^+ in 3 M HNO_3 for 12 h. All runs were conducted at S/L = 0.5, 300 rpm, and 30°C except for the thermodynamics experiments wherein adsorption runs were carried out at varied temperatures (40°C, 50°C, and 60°C).

$$Q_t = \frac{\left(C_0 - C_t\right)V}{m} \tag{4}$$

2.5. Sorbent characterization

A series of characterization techniques were performed on the most suitable resin to further investigate and correlate its properties with its Cs^+ uptake performance. Functional groups of synthesized materials were identified via Fourier transform infrared spectroscopy (FTIR) analysis (Thermo Scientific, Nicolet 4 iS5). Thermogravimetric analysis and differential scanning calorimetry were performed using a TGA-DSC unit (Mettler Toledo DSC 3, Australia). Surface morphology imaging and elemental mapping were carried out using a scanning electron microscope equipped with an energy-dispersive X-ray spectrometer (SEM-EDX, Hitachi S-3500N, Japan). Epoxy resin density was measured in water using a 25 mL pycnometer with a thermometer (Witeg, Germany) at 25°C equilibrated for 24 h prior to measurements. Swelling behavior was evaluated in terms of water uptake. The water uptake was gravimetrically estimated using Eq. (5) where w_1 is the dry weight of the epoxy resin and w_2 is its weight after soaking for 1 h in water [28].

$$\% W_{\text{uptake}} = \frac{\left(w_2 - w_1\right)}{w_1} \times 100 \tag{5}$$

3. Results and discussion

3.1. Fabrication of epoxy resins

The chemical structures of synthesized bis-epoxides BE1 and BE2 were confirmed by FTIR analysis (Fig. S1) whereas commercially available BE3 was used directly without further purification. All resins were formed by controlling the ratio of the BE component and the solvent DMSO (Table S1). When DMSO was added at higher portion (i.e. lower BE*n*/DMSO ratio), the reactants either remained in liquid form or produced gel-type/soft solids. This implies that the ability of the diamines and BEs to crosslink is influenced by the amount of solvent. Gel-type and soft solid resins were discarded as they could swell and physically disintegrate when applied as sorbents.

Increasing the BE*n*/DMSO ratio was more favorable to resin formation as the components reacted sufficiently, generating the desired linkages and producing the needed mechanical toughness as solid adsorbents. All resins were successfully formed at BE*n*/DMSO ratio (wt/wt) = 1.25 except for BE2-Ep which was obtained at 0.83 (Fig. 2a). The colors of the resins were affected by the type of BE used: those produced from BE1 were amber, from BE2 light yellow and from BE3 golden brown (Fig. 2a). The resins swell in water at different degrees based on water uptake measurements: BE1-Ep by 34.55%, BE2-Ep by 36.11% and BE3-Ep by 162.53%. These results suggest that the resins are hydrophilic and that two resins (BE1-Ep and BE2-Ep) prepared from two structurally-similar bis-epoxides swell minimally in water (Fig. 2b). These resins were directly tested in adsorption runs to select the most suitable adsorbent for Cs^+ in terms of capacity and selectivity using simulated HLLW feed in 3 M HNO_3.

3.2. Proposed mechanism of adsorption of Cs^+ to the epoxy resins

The sequestration mechanism of Cs^+ by epoxy resins prepared in this study can be ascribed mainly to electrostatic interactions with negatively charged moieties such as O and S atoms. The selectivity of the resins toward Cs^+ in the presence of other metal ions can be achieved by exploiting its physical and chemical properties. These properties include (1) having the largest ionic radius (1.81 Å) among metal ions in the target aqueous media; (2) having the lowest Gibb's free energy of dehydration (250 kJ mol^{-1}), which means that it is easiest to be freed from surrounding water molecules and acquire a bare or partially naked form which is often necessary for complex formation with ligands; and (3) being relatively softer than the other alkali metal ions (e.g. Na^+, K^+) which are usually its main interfering ions [29,30]. Size-induced selectivity might be exploited by using ligands that possess relatively large and wide coordination regions so that a large ion like Cs^+ can be conveniently accommodated while smaller interfering ions like Na^+ are sequestered with much difficulty due to geometric distortions that the ligand must undergo. Moreover, the inclusion of soft donor atoms like S in ligand design would result in preferential complexation with Cs^+ due to its relative softness as has been observed in sulfur-bearing Cs^+ sensors [31,32]. The operation of these selectivity factors was sought in the preparation of Cs^+-selective epoxy resins and appears to have been successfully achieved.

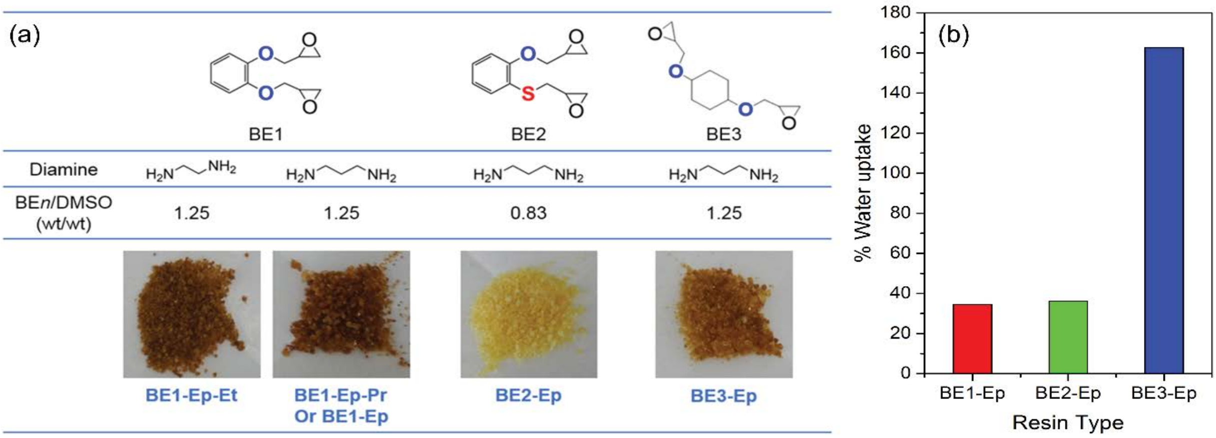

Fig. 2. (a) Epoxy resins produced as solid adsorbents by controlling the amount of DMSO solvent and (b) swelling test of the resins through % water uptake.

3.3. Resin screening through adsorption evaluation in simulated HLLW

The simulated feed contains metal ions including Na^+, Cr^{3+}, Ni^{2+}, Rb^+, Sr^{2+}, Cs^+ and Ba^{2+} that are typically present in acidic (3 M HNO_3) HLLW [27]. Results show that the performance of the resins may be linked to the structure and atomic composition of the BEs and diamine curing agent. The trends and correlations underlying the observations are discussed in the following subsections.

3.3.1. Effect of diamine curing agent

To observe the effect of the curing agent, two types of epoxy resins using BE1 as the bis-epoxide component were prepared: one with ethylenediamine (BE1-Ep-Et) and another with diaminopropane (BE1-Ep-Pr). The two amine curing agents possess the same set of functional groups and differ only in terms of the alkyl chain length, with diaminopropane being one alkyl carbon longer. The Q values of different metal ions in BE1-Ep-Et and BE1-Ep-Pr are shown in Fig. 3a. Despite the minimal difference in chain length, results show that BE1-Ep-Et prefers to adsorb Na^+ whereas BE1-Ep-Pr registers a marked preference for Cs^+ as further confirmed by their respective K_D values (Fig. 3b and c). This outcome can be explained by the difference in channel sizes created in the epoxy matrix when using these diamine linkers. Among the ions present in the feed, Cs^+ is the largest with r = 1.81 Å. Having been cured with a shorter diamine linker, BE1-Ep-Et permits the transport of small metal ions like Na^+ into its narrow channel spaces while the transport of large ions like Cs^+ and Rb^+ (r = 1.66 Å) is hindered. On the other hand, having been cured with a longer diamine linker, the channel spaces in BE1-Ep-Pr are wider and permit the permeation and coordination of Cs^+ with the oxygen and nitrogen atoms within the resin matrix. These results suggest that the length of the diamine linker plays a vital role in controlling the metal ion selectivity of epoxy resins.

The α value which is the ratio of the K_D of Cs^+ versus the K_D of other metal ions indicates the selectivity of the resin. The red dotted lines in Fig. 3b and c depict α = 1, which means that the resin has equal affinity towards the metal ion and Cs^+; α > 1 means the resin is selective towards Cs^+ versus the metal ion and α < 1 means it is more selective towards the metal ion relative to Cs^+. Between the two resins, BE1-Ep-Et has very low selectivity towards Cs^+ and is more selective towards other metal ions (α < 1) except for Rb^+. On the other hand, BE1-Ep-Pr is more selective towards Cs^+ than with the other metal ions (α > 1). These results confirm that diaminopropane is the more suitable curing agent for preparing Cs^+-selective epoxy resins. Henceforth, BE1-Ep-Pr is termed BE1-Ep for simplicity of discussion.

3.3.2. Effect of epoxide reactive arms opening

With diaminopropane as the appropriate curing agent, the effect of BE arm opening was studied next by comparing the adsorption capacities of epoxy resins BE1-Ep with BE3-Ep. BE1 has its oxygen donor atoms in ortho position whereas BE3 has its oxygens in para position. Thus, BE3 has a bigger epoxy arm opening than BE1. Generally higher Q values were observed in BE3-Ep compared with BE1-Ep (Fig. 4a). This outcome reinforces the idea that the capacity and selectivity for metal ions in the epoxy resins prepared in this study is primarily a function of the space-forming effects of the starting materials. It appears in fact that the effect of BE arm opening in creating accessible channels is more remarkable than the length of diamine curing agent.

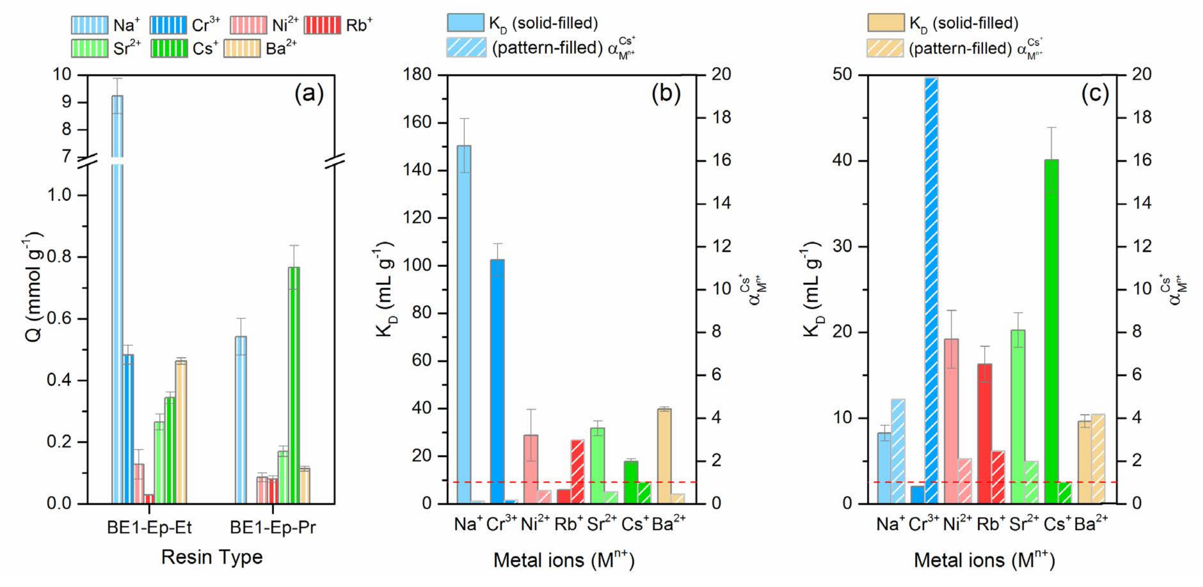

Fig. 3. Effect of the type of diamine curing agents on the performance of epoxy resins: (a) adsorption capacity of BE1-Ep-Et and BE1-Ep-Pr for various metal ions in simulated HLLW, (b) corresponding selectivity of BE1-Ep-Et in terms of K_D and α values for Cs^+ vs. other metal ions, and (c) corresponding selectivity of BE1-Ep-Pr in terms of K_D and α values for Cs^+ vs. other metal ions. [Conditions: S/L = 0.5, 300 rpm, 30°C, 12 h; simulated HLLW composition: Na^+ (66.04 mM), Cr^{3+} (4.96 mM), Ni^{2+} (4.52 mM), Rb^+ (5.01 mM), Sr^{2+} (8.50 mM), Cs^+ (19.50) and Ba^{2+} (11.89 mM) in 3 M HNO_3].

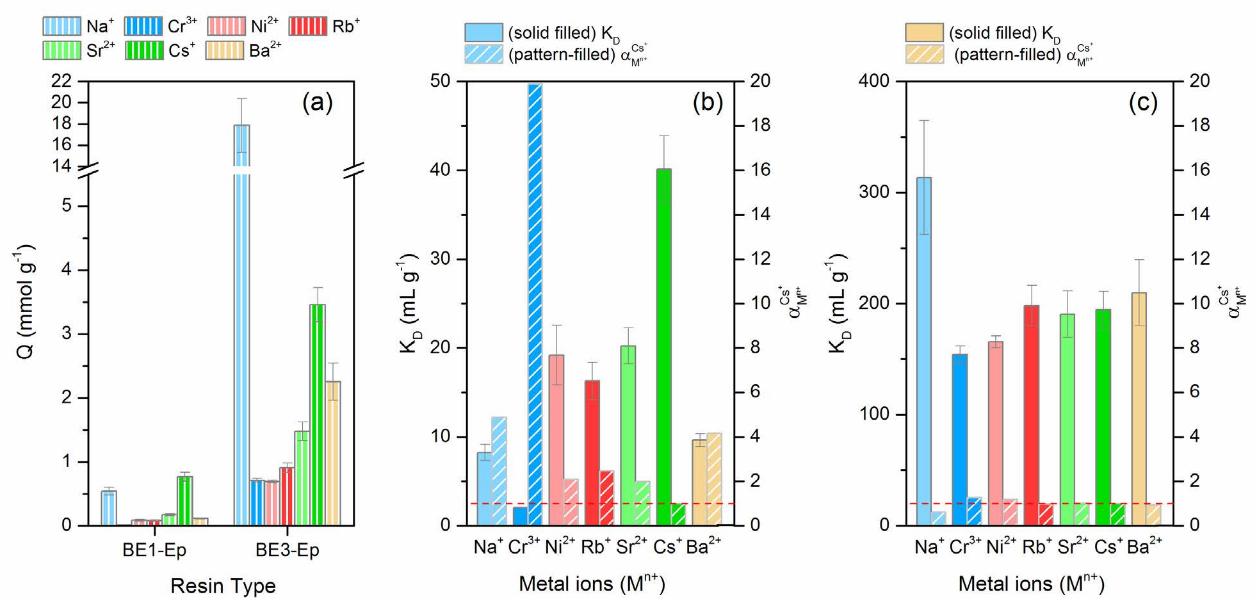

Fig. 4. Effect of BE with varying epoxide arm openings on the performance of epoxy resins: (a) adsorption capacity of BE1-Ep and BE3-Ep for various metal ions in simulated HLLW, (b) corresponding selectivity of BE1-Ep in terms of K_D and α values for Cs^+ vs. other metal ions, and (c) corresponding selectivity of BE3-Ep in terms of K_D and α values for Cs^+ vs. other metal ions. [Conditions: S/L = 0.5, 300 rpm, 30°C, 12 h; simulated HLLW composition: Na^+ (66.04 mM), Cr^{3+} (4.96 mM), Ni^{2+} (4.52 mM), Rb^+ (5.01 mM), Sr^{2+} (8.50 mM), Cs^+ (19.50) and Ba^{2+} (11.89 mM) in 3 M HNO_3].

The wide reactive arm opening of BE3 gave rise to ever wider channels in BE3-Ep that allow more ions to permeate the resin matrix, resulting in higher Q values. Unfortunately, all metal ions registered indiscriminately higher K_D values in BE3-Ep than in BE1-Ep, resulting in α values ~ 1 (Fig. 4b and c). This means that BE3-Ep has essentially equal preference for all metal ions in the feed. Moreover, Na^+ appears to be its most preferred ion (α < 1) (Fig. 4c). Thus, between the two resins, BE1-Ep remains to be the superior sorbent for Cs^+ considering its better selectivity towards Cs^+ and despite its relatively lower Q values than BE3-Ep.

3.3.3. Effect of coordinating atom

The effect of coordinating atom was investigated next by comparing the performance of resins containing two structurally similar bis-epoxides BE1 and BE2 which differ only in one donor atom. BE1 has two O as donor atoms whereas BE2 has one O and one S as donor atoms. Based on the Hard-soft-acid-base (HSAB) principle, S is a relatively "softer" donor atom than O. This means that BE2 is a "softer" ligand than BE1. It also implies that BE2 can form a stronger complex with "softer" ions or could be less accommodating to "hard" ions. Compared with other "hard" alkali metal ions like Na^+ and Rb^+, Cs^+ is considered relatively "soft" given its larger ionic size and higher polarizability [33]. Other ions present such as Ba^{2+}, Sr^{2+}, and Cr^{3+} are also known "hard" ions while Ni^{2+} is considered borderline "soft" [34].

The presence of S atoms in BE2-Ep had a very minor effect on the Q and K_D of Cs^+ but it clearly reduced the Q and K_D values of most interfering metal ions which are relatively "harder" than Cs^+ (Fig. 5a–c). The only exception was Ni^{2+} which had a slightly higher Q and K_D in BE2-Ep than in BE1-Ep since it is the "softest" metal ion present in the feed. But given its low initial concentration, its overall uptake is also low. In effect, results indicate that a slight modification in the donor atoms present in the resin can palpably alter the overall selectivity. With the reduction of K_D values of most interfering metal ions, the α values of BE2-Ep are remarkably better than those of BE1-Ep, especially for Na^+, which is the major constituent of the simulated HLLW feed. Thus, among the resins tested, BE2-Ep is the most suitable sorbent both in terms of its capacity and selectivity towards Cs^+.

3.4. BE2-Ep as a Cs^+-sorbent

BE2-Ep appears to be the most superior Cs^+ sorbent among the epoxy resins prepared in this study. Aside from space-forming effects of the benzene moiety in BE2 and the presence of the relatively "softer" donor atom S, the preference of BE2-Ep for Cs^+ might additionally be explained in terms of the interaction of benzene moieties in BE2 with the metal ions present in the aqueous feed. It has been shown in various studies that the aromatic moiety interacts preferentially with Cs^+ due to its low dehydration energy requirement, and that the inclusion of as many benzene moieties in ligand design can prove advantageous [35,36]. In BE2-Ep, coordination of Cs^+ with the oxygen, sulfur and nitrogen atoms may have been enhanced and stabilized further by its rich collection of aromatic groups. As such, further evaluation of the material properties and adsorption behavior of BE2-Ep was performed. Results from this evaluation are discussed in the following subsections.

3.4.1. Characterization of BE2-Ep

The glassy yellow BE2-Ep has an apparent density of 1.394 g cm^{-3} (Fig. 6a). SEM images show that the resin surface has rough and smooth features with no visible pores (Fig. 6b). This is expected since the pore channels created between linkages are projected to be approximately 9 Å measured from the minimized energy chemical structure of BE2-Ep resin using MM2 force field method in Chem3D® (Fig. 6c). This pore channel dimension is too small to be seen in SEM images. Meanwhile, elemental mapping on the resin surface reveals the rich presence of C, N, O, and S

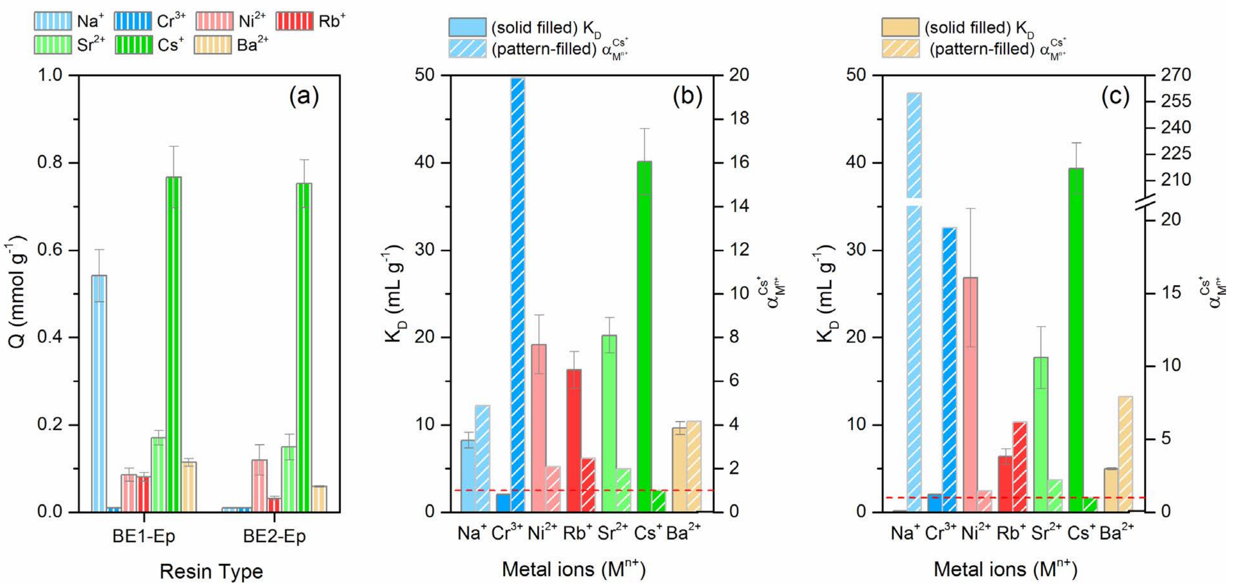

Fig. 5. Effect of BE donor atoms on the performance of epoxy resins: (a) adsorption capacity of BE1-Ep and BE2-Ep for various metal ions in simulated HLLW, (b) corresponding selectivity of BE1-Ep in terms of K_D and α values for Cs^+ vs. other metal ions, and (c) corresponding selectivity of BE2-Ep in terms of K_D and α values for Cs^+ vs. other metal ions. [Conditions: S/L = 0.5, 300 rpm, 30°C, 12 h; simulated HLLW composition: Na^+ (66.04 mM), Cr^{3+} (4.96 mM), Ni^{2+} (4.52 mM), Rb^+ (5.01 mM), Sr^{2+} (8.50 mM), Cs^+ (19.50) and Ba^{2+} (11.89 mM) in 3 M HNO_3].

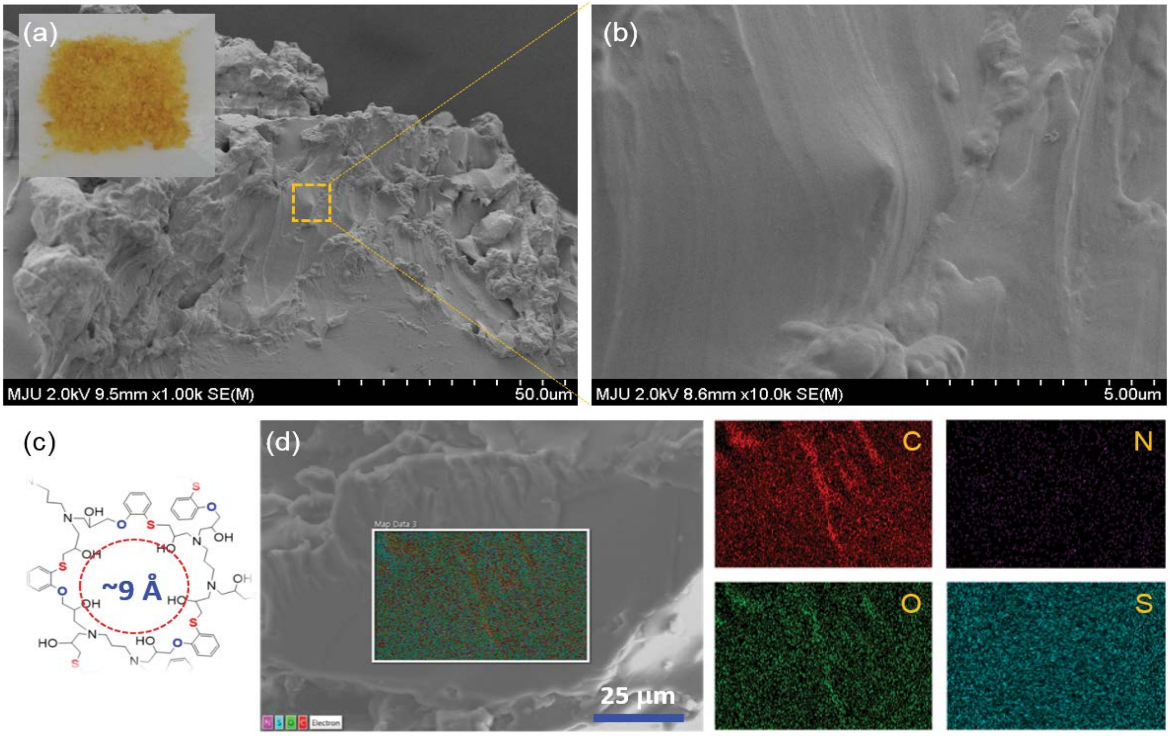

Fig. 6. Physico-chemical characterization of BE2-Ep: (a) optical and SEM image of BE2-Ep granules, (b) SEM image at higher magnification, (c) pore channel structure of BE2-Ep and its estimated dimension, and (d) surface elemental mapping of BE2-Ep.

atoms which coincides well with the composition of BE2-Ep (Fig. 6d).

Further examination of BE2-Ep via FTIR reveals the presence of –OH and –NH functionalities (3,242 cm^{-1}) which are the result of the addition reaction involving the reactive oxirane rings and primary amines (Fig. 7a). Vibrations related to aromatic ring stretching appear as two peaks in 1,712 and 1,578 cm^{-1}. Other distinguishing peaks are the C–N (1,441 cm^{-1}), C–O (1,069 and 1,038 cm^{-1}), and C–S (682 cm^{-1}) stretching vibrations. The observed peaks confirm the successful linking of BE2 with the diaminopropane curing agent.

BE2-Ep appears to be thermally stable up to 250°C before it starts to drastically decompose at 270°C. Majority of its mass loss (~8%) at <150°C can be mainly attributed to evaporation of adsorbed water (Fig. 7b). The DSC profile of BE2-Ep shows that the resin starts to transition into a rubbery state at about T_g = 90.35°C (inset, Fig. 7b). This means that within the adsorption temperatures tested, the resin maintains its solid, glassy property since it undergoes minimal swelling in water (W_{uptake} = 36.11%).

3.4.2. Adsorption isotherm

The adsorption capacity of BE2-Ep for Cs$^+$ in acidic (3 M HNO$_3$) aqueous solutions of Cs$^+$ (65–1,340 mg L^{-1}) was determined to estimate its $Q_{\max}$. Results are plotted in Fig. 8a along with non-linear fitting curves generated using selected isotherm models [Eqs. (6)–(10)] listed in Table 1.

The experimental adsorption capacity (Q_{expt}) of BE2-Ep for Cs$^+$ is about 1.004 mmol g^{-1} (133.5 mg g^{-1}) which is slightly better than the highest adsorption capacity (0.96 mmol g^{-1} at 3 M HNO$_3$) reported for calixarene-based sorbents [21]. The Langmuir, Redlich–Peterson, Temkin and Hill isotherm models show good approximations of the adsorption data, registering R^2 values near unity (Table 2). The very high R^2 value obtained with the Redlich–Peterson model suggests that the adsorption of Cs$^+$ by BE2-Ep embodies assumptions

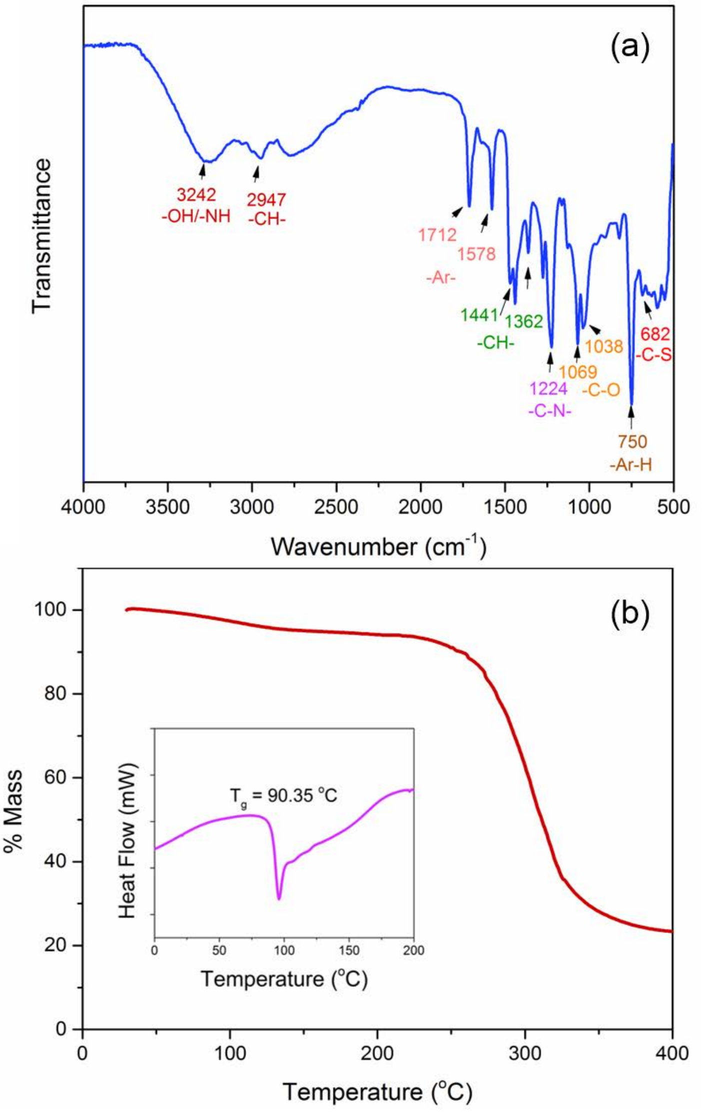

Fig. 7. Chemical and thermogravimetric analyses of BE2-Ep: (a) FTIR spectrum and (b) TGA-DSC curves.

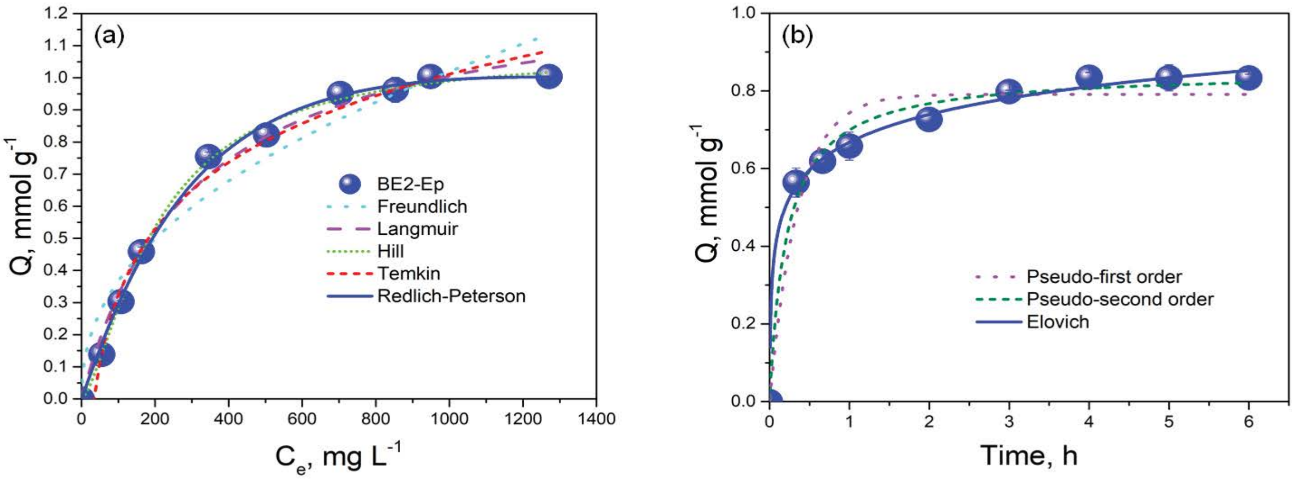

Fig. 8. Non-linear isotherm and kinetics plots for the adsorption of Cs$^+$ by BE2-Ep. [Isotherm conditions: C_0 ~65–1,340 mg L^{-1}, 3 M HNO$_3$, S/L = 0.5, 300 rpm, 30°C, 12 h; kinetic conditions: C_0 ~570 mg L^{-1}, 3 M HNO$_3$, S/L = 0.5, 300 rpm, 30°C].

Table 1
Isotherm models used for the adsorption of Cs$^+$ by BE2-Ep

Model	Equation	Parameters	Equation
Freundlich	$q_e = K_F C_e^{1/n}$	n = Freundlich adsorption intensity; K_F = Freundlich constant for adsorption energy	(6)
Langmuir	$q_e = \frac{q_m K_L C_e}{1 + K_L C_e}$	q_m = maximum adsorption capacity; K_L = Langmuir constant for adsorption energy	(7)
Redlich–Peterson	$q_e = \frac{K_{RP} C_e}{1 + \alpha_{RP} C_e^{\beta}}$	α_{RP}, β, and K_{RP} are Redlich–Peterson isotherm constants	(8)
Hill	$q_e = \frac{q_m C_e^{n_H}}{K_H + C_e^{n_H}}$	q_m = maximum monolayer adsorption capacity; n_H = Hill cooperativity binding coefficient; K_H = Hill isotherm constant	(9)
Temkin	$q_e = \frac{RT}{b} \ln\left(K_T C_e\right)$	b = Temkin isotherm constant related to the heat of sorption; K_T = Equilibrium binding constant	(10)

represented by both Langmuir (monolayer adsorption) and Freundlich (heterogenous surface) models [37], unlike the calixarene-based sorbents that usually adhere to the Langmuir model [17–19,21]. Operationally, this means that BE2-Ep works best when the initial concentration of Cs$^+$ in the feed is high. In terms of predicting the maximum adsorption capacity, the Hill isotherm yields a value of 1.049 mmol g^{-1} (139.5 mg g^{-1}) which is very near the experimental value.

Assuming that Cs$^+$ coordinates with all the O, S, and N atoms of the resin, the theoretical adsorption capacity (Q_{theo}) of BE2-Ep is approximately 1.52 mmol g^{-1}. The lower value of Q_{expt} (~66% Q_{theo}) might be partly explained by the lack of porosity of the resin which limits sorbate access into the innermost regions of the resin matrix, and partly by the presence of a large concentration of H$_3$O$^+$ in the feed which may have occupied some of the coordination sites.

3.4.3. Adsorption kinetics

The rate of Cs$^+$ uptake of BE2-Ep was studied using three kinetic models listed in Table 3, which include the pseudo-first-order [Eq. (11)], pseudo-second-order [Eq. (12)], and the Elovich equation [Eq. (13)]. The parameter α_E (mmol g^{-1} h^{-1}) is the initial adsorption rate related to surface energy whereas β_E (g mmol^{-1}) is the desorption constant related to the activation energy in the Elovich model. Adsorption data are plotted in Fig. 8b along with non-linear fitting curves. Kinetic model parameters from the fitting results are summarized in Table 4.

Based on the R^2 values, the adsorption of Cs$^+$ by BE2-Ep is best embodied by the Elovich equation which means that the sequestration mechanism occurs via chemisorption [38]. The constant α_E which is the initial adsorption rate has a value greater than that of β_E which is a desorption constant.

This means that adsorption is favored over desorption during the sequestration process. Saturation is essentially achieved after 4 h of adsorption run.

The uptake rate of BE2-Ep for Cs^+ (5.458 g mmol^{-1} h^{-1}) estimated using the pseudo-second-order model is lower than those of calixarene-based sorbents. For example, calix[4] arene impregnated in mesoporous silica [39] and calix[4] arene-crown-6 tethered on mesoporous carbon [21] deliver uptake rates of 39.102 and 4,812 g mmol^{-1} h^{-1}, respectively. The relatively slower kinetics in BE2-Ep might be ascribed to limited transport of Cs^+ into the inner resin matrix, especially after its surface layer has reached saturation. On the other hand, the porous nature of calixarene-based sorbents provides easy access of Cs^+ onto sorption sites.

Table 2
Non-linear isotherm fitting parameters for the sequestration of Cs^+ by BE2-Ep

Isotherm model	Value
Freundlich	
K_F, (mmol g^{-1})(L mg^{-1})$^{1/n}$	0.20
$1/n$	0.46
R^2	0.853
Langmuir	
K_L, (L mg^{-1})	0.00205
q_m, (mmol g^{-1})	1.40 ± 0.12
R^2	0.953
Redlich–Peterson	
K_{RP}, (mmol g^{-1})(L mg^{-1})	0.00183
α_{RP}	3.65
β	1.88
R^2	0.989
Hill	
q_m, (mmol g^{-1})	1.049 ± 0.021
n_H	2.25
$K_H, \left(\text{mg L}^{-1}\right)^{n_H}$	3.55 × 105
R^2	0.993
Temkin	
K_T, (L mg^{-1})	0.029
b, (J mol^{-1})	8392
R^2	0.989
$q_{\text{experimental}}$, (mmol g^{-1})	1.004

3.4.4. Adsorption thermodynamics

BE2-Ep was subjected to equilibrium adsorption runs at different temperatures to determine the thermodynamic parameters of the adsorption process. It was found that BE2-Ep adsorbs more Cs^+ as the temperature is increased (Fig. 9a), contrary to findings with calixarene-based sorbents for which enhanced ligand degradation in 3 M HNO_3 occurred with increasing temperature leading to lower adsorption capacities [19–21,40] and with ion-imprinted polymer which tend to undergo deformation and warping of ion-imprinted coordination sites as the polymer undergoes thermal expansion [14]. For BE2-Ep, higher adsorption capacities with increasing temperature was probably the result of increased interactive collisions between sorbent and sorbate. The endothermic nature of the adsorption process is further confirmed from $\Delta H°$ obtained from the linearized van't Hoff equation [Eq. (14), Fig. 9b] which registered a positive value (Table 5). Moreover, the adsorption process is spontaneous ($\Delta G° < 0$), accompanied by increased disorder at the solute–sorbate interface ($\Delta S° > 0$) [41].

Table 4
Non-linear kinetic fitting parameters for the sequestration of Cs^+ by BE2-Ep

Kinetic model	Value
Pseudo-first-order	
k_1, (h^{-1})	2.809
R^2	0.953
Pseudo-second-order	
k_2, (g mmol^{-1} h^{-1})	5.458
q_m, (mmol g^{-1})	0.850 ± 0.020
R^2	0.986
Elovich	
α_E (mmol g^{-1} h^{-1})	66.721
β_E (g mmol^{-1})	9.692
R^2	0.997

Table 3
Kinetic models used for the adsorption of Cs^+ by BE2-Ep

Model	Equation	Parameters	Equation
Pseudo-first-order	$q_t = q_e\left(1-e^{-k_1 t}\right)$	k_1 = rate constant (h^{-1})	(11)
Pseudo-second-order	$q_t = \dfrac{k_2 q_e^2 t}{1+k_2 q_e t}$	k_2 = rate constant (g mmol^{-1} h^{-1})	(12)
Elovich	$q_t = \dfrac{\ln\left(\alpha_E \beta_E t\right)}{\beta_E}$	α_E and β_E are Elovich model constants	(13)

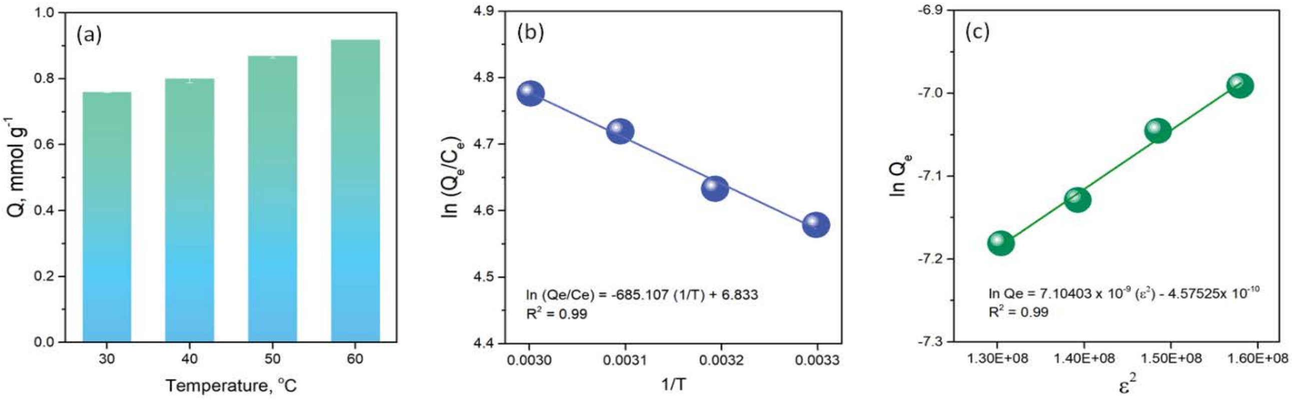

Fig. 9. (a) Adsorption capacity for Cs^+ by BE2-Ep at different temperatures; and the linearized plot of the (b) van't Hoff and (c) Dubinin–Radushkevich equations for the adsorption of Cs^+ by BE2-Ep [Conditions: C_0 ~1,330 mg L^{-1}, 3 M HNO_3, S/L = 0.5, 300 rpm, 30°C, 4 h].

Table 5
Thermodynamic parameters for the adsorption of Cs^+ by BE2-Ep at different temperatures [Conditions: C_0 = 330 ppm, 250 rpm, S/L = 0.5, 3 M HNO_3, 4 h]

Temperature, °C	$\Delta S°$, J mol^{-1} K^{-1}	$\Delta H°$, kJ mol^{-1}	$\Delta G°$, kJ mol^{-1}
30	56.807	5.696	–11.540
40	56.807	5.696	–12.061
50	56.807	5.696	–12.679
60	56.807	5.696	–13.228

$$\ln\frac{Q_e}{C_e}=\frac{\Delta S°}{R}-\frac{\Delta H^0}{RT} \tag{14}$$

Adsorption data for examining the effect of temperature were also plotted using the Dubinin–Radushkevich (D–R) isotherm to further evaluate whether the adsorption process occurs by physical or chemical modes through the value of the mean free energy (E) of adsorption. If E is less than 8 kJ mol^{-1}, the sorption process is by physical mode; if E is between 8 and 16 kJ mol^{-1}, the process proceeds via chemisorption [42,43]. The D–R isotherm is expressed in Eqs. (15)–(17).

$$\ln q_e=\ln q_m-\beta\varepsilon^2 \tag{15}$$

$$\varepsilon=RT\ln\left(1+\frac{1}{C_e}\right) \tag{16}$$

$$E=\frac{1}{\sqrt{-2\beta}} \tag{17}$$

The linear plot of $\ln q_e$ against the Polanyi potential energy (ε^2) is shown in Fig. 9c. A high correlation coefficient (R^2 = 0.99) was obtained which means that β, α constant related to the mean free energy of adsorption per mole of adsorbate, can be taken to be -7.104×10^{-9} mol^2 J^{-2}. This corresponds to a mean free energy of adsorption of 8.4 kJ mol^{-1} which signifies chemisorption. This is consistent with the assumption that the adsorption of Cs^+ by BE2-Ep is the combined effects of complexation with O, S, and N atoms, and cation-π interactions involving the benzene moieties of the BE2 component.

3.4.5. Comparison with other Cs^+ sorbents applied in acidic media

The adsorption of Cs^+ in acidic media had so far been achieved only with the use of calixarene-based sorbents. A compilation of the adsorption performance data of these sorbents have been summarized in Table 6, along with those of BE2-Ep so that meaningful comparisons can be made. From the table, almost all calixarene-based sorbents have low ligand loading (<0.50 mmol g^{-1}) on their respective solid supports. Consequently, low adsorption capacities (<30 mg g^{-1}) were achieved. On the other hand, BE2-Ep might be regarded to possess a considerably higher theoretical ligand load (1.52 mmol g^{-1} as mentioned in section 3.4.2) than the calixarene-based sorbents listed in Table 6 since the bulk resin is rich in O, S, N, and aromatic moieties which interact with Cs^+. Although the maximum Q = 133.5 mg g^{-1} obtained in BE2-Ep is lower than its theoretical ligand loading, it is still remarkably higher than the Q of most calixarene-based sorbents. However, in terms of kinetics, BE2-Ep takes a longer time to reach equilibrium compared with most calixarene-based sorbents which possess porous structures that facilitate fast diffusion of Cs^+ to the binding sites. As such, it is recommended for future improvement of BE2-Ep to enhance its porosity (i.e. using appropriate porogen) if faster Cs^+ uptake rate is desired. Nevertheless, the overall performance of BE2-Ep is comparable with that of calixarene-based sorbents but with the added benefits of simpler preparation and cheaper production. For its intended application, BE2-Ep can be employed as a single-use sorbent to pre-concentrate Cs^+ from acidic HLLW. The Cs^+-loaded BE2-Ep can then be separated from the HLLW and stored in specialized vessels to facilitate the

Table 6
Summary of adsorption performance of reported Cs^+ sorbents applied in acidic media

A. Calix-arene-based sorbents	Entry	Ligand	Ligand load, mmol g^{-1}	Q_{theo}, mg Cs^+ g^{-1} sorbent	Q_{max} from best isotherm model, mg g^{-1}	Acid condition	S/L (g L^{-1})	Optimal contact time	Reference
Polymer-supported	1	1,3-calix[4]bis-o-benzo-crown-6 (“BC6B”)	0.017	2.23	N/A	<=1 M HNO_3	N/A (column operation)	N/A	[44]
	2	25,27-bis(iso-propyloxy)calix[4]arene-26,28-crown-6	0.469	62.38	N/A	4 M HNO_3	50	120 min	[45]
	3	25,27-bis(1-n-propoxy)-calix[4]26,28-crown-6 (BnPC6)	0.173	22.99	19.68 (Langmuir)	3–4 M HNO_3	50	60 min	[19]
Polymer-modified porous silica support	4	1,3-[(2,4-diethyl-heptylethoxy)oxy]-2,4-crown-6-calix[4]arene (Calix[4]arene-R14)	0.230	30.55	N/A	N/A	50	30 min	[46]
	5	Calix[4]arene-R14	0.230	30.55	N/A	3 M HNO_3	50	180 min	[47]
	6	25,27-bis(iso-propyloxy)calix[4]arene-26,28-crown-6 (BiPCalix[4]C6)	N/A	N/A	N/A	3 M HNO_3	50	120 min	[48]
	7	Calix[4]arene-R14	N/A	N/A	28 (not modelled)	4 M HNO_3	50	120 min	[20]
	8	Calix[4]arene-R14	N/A	N/A	25 (Langmuir)	4 M HNO_3	50	5 h	[17]
	9	Calix[4]arene-R14	N/A	N/A	N/A	3 M HNO_3	5	Not reported	[7]
	10	Calix[4]arene-R14	0.156	20.80	20.75 (Langmuir)	0.5 M HNO_3	5 to 20	Not reported	[40]
	11	Calix[4]arene-R14	0.244	32.50	19.95 (Langmuir)	3 M HNO_3	50	120 min	[39]
	12	Di(1-hexyloxy)-2,4-crown-6-calix[4]arene (C7C6Calix)	0.231	30.72	16.40 (Langmuir)	1 M HNO_3	50	125 min	[18]
Mesoporous carbon support	13	Calix[4]arene-crown-6	Not reported	N/A	128.06 (Langmuir)	3 M HNO_3	1	60 min	[21]
B. Epoxy resin (BE2-Ep)	14	Oxygen-, sulfur-, and benzene-bearing bis-epoxide cured with diaminopropane	1.52	202.16	139.5 (Hill) 133.5 (Expt’l)	3 M HNO_3	0.5	4 h	This work

natural radioactive decay process. Overall results show the potential application of BE2-Ep for Cs^+ sequestration.

4. Conclusions

New types of epoxy resins with inherent adsorptive capacity and selectivity for Cs^+ in highly oxidizing and acidic conditions were first prepared and reported in this study. The resins were synthesized via epoxide ring opening reaction of bis-epoxides and diamine curing agents. It was found that the proper combination of bis-epoxide and diamine linker could result in the permeation and adsorption of Cs^+ into the resin matrix, which means that the creation of adequately sized channel spaces is vital to the selective sequestration of Cs^+ by epoxy resins. As such, bis-epoxides with electronegative atoms located in ortho position in a central benzene moiety and cured with diaminopropane appear to provide the desired Cs^+-selective resins. One such resin (BE2-Ep) which contains both S and O donor atoms showed the highest selectivity towards Cs^+ versus interfering metal ions present in HLLW. This means that, aside from having adequately sized channel spaces, Cs^+ selectivity can be further enhanced in epoxy resins by making them "softer" through use of sulfur-bearing bis-epoxides. BE2-Ep registers an experimental adsorption capacity of 1.004 mmol g^{-1} in 3 M HNO_3 which is higher than the best performing calixarene-based sorbent under the same acid conditions. BE2-Ep stands among the very few set of Cs^+-selective sorbents that can be applied in highly acidic HLLW prior to long-term storage of radioactive wastes.

Declaration of interests

The authors declare that they have no known competing financial interests or personal relationships that could have influenced the work reported in this paper.

Acknowledgment

This work was supported by the National Research Foundation of Korea (NRF) grant funded by the Ministry of Science and ICT (2020R1A2C1003560, 2021R1A2C2093746, and 2021R1H1A2008284), Basic Science Research Program through the Ministry of Education (2020R1A6A1A03038817), and by the Korea Institute of Technology Evaluation and Planning (KETEP) funded by the Ministry of Trade, Industry & Energy (MOTIE No. 20194010201750).

References

[1] H.-H. Rogner, World outlook for nuclear power, Energy Strategy Rev., 1 (2013) 291–295.

[2] H. Khatib, IEA World Energy Outlook 2011 –A Comment, Energy Policy, 48 (2012) 737–743.

[3] F.J. Maringer, J. Suráň, P. Kovář, B. Chauvenet, V. Peyres, E. García-Toraño, M.L. Cozzella, P. De Felice, B. Vodenik, M. Hult, U. Rosengård, M. Merimaa, L. Szücs, C. Jeffery, J.C.J. Dean, Z.Z. Tymiński, D. Arnold, R. Hinca, G. Mirescu, Radioactive waste management: review on clearance levels and acceptance criteria legislation, requirements and standards, Appl. Radiat. Isot., 81 (2013) 255–260.

[4] B.R. Figueiredo, S.P. Cardoso, I. Portugal, J. Rocha, C.M. Silva, Inorganic ion exchangers for cesium removal from radioactive wastewater, Sep. Purif. Rev., 47 (2018) 306–336.

[5] H. Yang, M. Luo, L. Luo, H. Wang, D. Hu, J. Lin, X. Wang, Y. Wang, S. Wang, X. Bu, P. Feng, T. Wu, Highly selective and rapid uptake of radionuclide cesium based on robust zeolitic chalcogenide via stepwise ion-exchange strategy, Chem. Mater., 28 (2016) 8774–8780.

[6] P.A. Haas, A review of information on ferrocyanide solids for removal of cesium from solutions, Sep. Sci. Technol., 28 (1993) 2479–2506.

[7] Z. Chen, Y. Wu, Y. Wei, Cesium removal from high level liquid waste utilizing a macroporous silica-based calix[4]arene-R14 adsorbent modified with surfactants, Energy Procedia, 39 (2013) 319–327.

[8] C. Xu, J. Wang, J. Chen, Solvent extraction of strontium and cesium: a review of recent progress, Solvent Extr. Ion Exch., 30 (2012) 623–650.

[9] S.-C. Jang, S.-M. Kang, Y. Haldorai, K. Giribabu, G.-W. Lee, Y.-C. Lee, M.S. Hyun, Y.-K. Han, C. Roh, Y.S. Huh, Synergistically strengthened 3D micro-scavenger cage adsorbent for selective removal of radioactive cesium, Sci. Rep., 6 (2016) 38384, doi: 10.1038/srep38384.

[10] J. Qian, J. Ma, W. He, D. Hua, Facile synthesis of Prussian blue derivate-modified mesoporous material via photoinitiated thiolene click reaction for cesium adsorption, Chem. Asian J., 10 (2015) 1738–1744.

[11] H. Faghihian, M. Moayed, A. Firooz, M. Iravani, Evaluation of new magnetic zeolite composite for removal of Cs^+ and Sr^{2+} from aqueous solutions, kinetic, equilibrium and thermodynamic studies, C.R. Chim., 17 (2014) 108–117.

[12] M.J. Manos, K. Chrissafis, M.G. Kanatzidis, Unique pore selectivity for Cs^+ and exceptionally high NH_4^+ exchange capacity of the chalcogenide material $K_6Sn[Zn_4Sn_4S_{17}]$, J. Am. Chem. Soc., 128 (2006) 8875–8883.

[13] J.L. Mertz, Z.H. Fard, C.D. Malliakas, M.J. Manos, M.G. Kanatzidis, Selective removal of Cs^+, Sr^{2+} and Ni^{2+} by $K_{2x}Mg_xSn_{3-x}S_6$ (x = 0.5–1) (KMS-2) relevant to nuclear waste remediation, Chem. Mater., 25 (2013) 2116–2127.

[14] Z. Zhang, X. Xu, Y. Yan, Kinetic and thermodynamic analysis of selective adsorption of Cs(I) by a novel surface whisker-supported ion-imprinted polymer, Desalination, 263 (2010) 97–106.

[15] H. Iwasaki, M. Yoshikawa, Molecularly imprinted polyacrylonitrile adsorbents for the capture of Cs^+ ions, Polym. J., 48 (2016) 1151–1156.

[16] M. Shamsipur, H.R. Rajabi, Flame photometric determination of cesium ion after its preconcentration with nanoparticles imprinted with the cesium-dibenzo-24-crown-8 complex, Microchim. Acta, 180 (2013) 243–252.

[17] A. Zhang, Z. Chai, Adsorption property of cesium onto modified microporous silica-calix[4]arene-crown based supramolecular recognition materials, Ind. Eng. Chem. Res., 51 (2012) 6196–6204.

[18] A. Zhang, C. Chen, Y. Ji, S. Liu, S. Guo, Uptake of cesium and some typical metals onto hybrid calix[4]crown adsorbent with silica carrier by host-guest recognition, J. Chem. Eng. Data, 63 (2018) 1578–1587.

[19] A. Zhang, Y. Wang, J. Li, Cesium and strontium uptake utilizing a new ternary solid-state supramolecular adsorbent under a framework of group partitioning, J. Chem. Eng. Data, 62 (2017) 1440–1447.

[20] Y. Wu, S.-Y. Kim, D. Tozawa, T. Ito, T. Tada, K. Hitomi, E. Kuraoka, H. Yamazaki, K. Ishii, Study on selective separation of cesium from high level liquid waste using a microporous silica-based supramolecular recognition absorbent, J. Radioanal. Nucl. Chem., 293 (2012) 13–20.

[21] Q. Tao, X. Wang, D. Huang, K. Prabaharan, Y. Dai, Adsorption of cesium from aqueous solution of highly concentrated nitric acid using supermolecule/ordered mesoporous carbon composite, Water Air Soil Pollut., 229 (2018) 361, doi: 10.1007/s11270-018-4016-6.

[22] N.A. St. John, G.A. George, Diglycidyl amine-epoxy resin networks: kinetics and mechanisms of cure, Prog. Polym. Sci., 19 (1994) 755–795.

[23] G. Yang, S.-Y. Fu, J.-P. Yang, Preparation and mechanical properties of modified epoxy resins with flexible diamines, Polymer, 48 (2007) 302–310.

[24] J. Wan, C. Li, Z.-Y. Bu, C.-J. Xu, B.-G. Li, H. Fan, A comparative study of epoxy resin cured with a linear diamine and a branched polyamine, Chem. Eng. J., 188 (2012) 160–172.

[25] R.E.C. Torrejos, G.M. Nisola, H.S. Song, L.A. Limjuco, C.P. Lawagon, K.J. Parohinog, S. Koo, J.W. Han, W.-J. Chung, Design of lithium selective crown ethers: synthesis, extraction and theoretical binding studies, Chem. Eng. J., 326 (2017) 921–933.

[26] R.E.C. Torrejos, G.M. Nisola, S.H. Min, J.W. Han, S. Koo, K.J. Parohinog, S. Lee, H. Kim, W.-J. Chung, Aqueous synthesis of 14–15 membered crown ethers with mixed O, N and S heteroatoms: experimental and theoretical binding studies with platinum-group metals, ChemPlusChem, 84 (2019) 210–221.

[27] D. Parajuli, K. Hirota, Recovery of palladium using chemically modified cedar wood powder, J. Colloid Interface Sci., 338 (2009) 371–375.

[28] Z. Zhang, G. Zhang, Y. Zhang, Z. Wang, D. Yu, X. Hu, C. Hu, X. Tang, Mechanical properties, water swelling behavior, and morphology of swellable rubber compatibilized by PVA-g-PBA, Polym. Eng. Sci., 44 (2004) 72–78.

[29] E.R. Nightingale Jr., Phenomenological theory of ion solvation. Effective radii of hydrated ions, J. Phys. Chem., 63 (1959) 1381–1387.

[30] Y. Marcus, Thermodynamics of solvation of ions. Part 5.—Gibbs free energy of hydration at 298.15 K, J. Chem. Soc., Faraday Trans., 18 (1991) 2995.

[31] Y. Choi, H. Kim, J.K. Lee, S.H. Lee, H.B. Lim, J.S. Kim, Cesium ion-selective electrodes based on 1,3-alternate thiacalix[4] biscrown-6,6, Talanta, 64 (2004) 975–980.

[32] R. Bereczki, V. Csokai, A. Grun, I. Bitter, K. Toth, Crown bridged thiacalix[4]arenes as cesium-selective ionophores in solvent polymeric membrane electrodes, Anal. Chim. Acta, 569 (2006) 42–49.

[33] H. Yang, M. Luo, L. Luo, H. Wang, D. Hu, J. Lin, X. Wang, Y. Wang, S. Wang, X. Bu, P. Feng, T. Wu, Highly selective and rapid uptake of radionuclide cesium based on robust zeolitic chalcogenide via stepwise ion-exchange strategy, Chem. Mater., 28 (2016) 8774–8780.

[34] H. Xu, D.C. Xu, Y. Wang, Natural indices for the chemical hardness/softness of metal cations and ligands, ACS Omega, 2 (2017) 7185–7193.

[35] R. Kumpf, D. Dougherty, A mechanism for ion selectivity in potassium channels: computational studies of cation-pi interactions, Science, 261 (1993) 1708–1710.

[36] F. Pichierri, Cs^+-π interactions and the design of macrocycles for the capture of environmental radiocesium (Cs-137): DFT, QTAIM, and CSD studies, Theor. Chem. Acc., 137 (2018) 118, doi: 10.1007/s00214-018-2298-9.

[37] M.A. Al-Ghouti, D.A. Da'ana, Guidelines for the use and interpretation of adsorption isotherm models: a review, J. Hazard. Mater., 39 (2020) 122383, doi: 10.1016/j.jhazmat.2020.122383.

[38] T.A. Khan, S.A. Chaudhry, I. Ali, Equilibrium uptake, isotherm and kinetic studies of Cd(II) adsorption onto iron oxide activated red mud from aqueous solution, J. Mol. Liq., 202 (2015) 165–175.

[39] Y. Wu, X. Zhang, S.-Y. Kim, Y. Wei, Simultaneous separation and recovery of Cs(I) and Sr(II) using a hybrid macrocyclic compound loaded adsorbent. Kinetic, equilibrium and dynamic adsorption studies, J. Nucl. Sci. Technol., 12 (2016) 1968–1977.

[40] Z. Chen, Y. Wu, Y. Wei, The effect of temperature and γ-ray irradiation on silica-based calix[4]arene-R14 adsorbent modified with surfactants for the adsorption of cesium from nuclear waste solution, Radiat. Phys. Chem., 103 (2014) 222–226.

[41] C.P. Lawagon, G.M. Nisola, J. Mun, A. Tron, R.E.C. Torrejos, J.G. Seo, H. Kim, W.J. Chung, Adsorptive Li^+ mining from liquid resources by H_2TiO_3: equilibrium, kinetics, thermodynamics, and mechanisms, J. Ind. Eng. Chem., 35 (2016) 347–356.

[42] U. Baig, R.A.K. Rao, A.A. Khan, M.M. Sanagi, M.A. Gondal, Removal of carcinogenic hexavalent chromium from aqueous solutions using newly synthesized and characterized polypyrrole–titanium(IV)phosphate nanocomposite, Chem. Eng. J., 280 (2015) 494–504.

[43] A. Babarinde, K. Ogundipe, K.T. Sangosanya, B.D. Akintola, A.O.E. Hassan, Comparative study on the biosorption of Pb(II), Cd(II) and Zn(II) using Lemon grass (*Cymbopogan citratus*): kinetics, isotherms and thermodynamics, Chem. Int., 2 (2016) 89–102.

[44] M.L. Dietz, D.D. Ensor, B. Harmon, S. Seekamp, Separation and preconcentration of cesium from acidic media by extraction chromatography, Sep. Sci. Technol., 41 (2006) 2183–2204.

[45] C. Xiao, A. Zhang, Z. Chai, Synthesis and characterization of a new polymer-based supramolecular recognition material and its adsorption for cesium, Solvent Extr. Ion Exch., 30 (2012) 17–32.

[46] A. Zhang, E. Kuraoka, M. Kumagai, Development of the chromatographic partitioning of cesium and strontium utilizing two macroporous silica-based calix[4]arene-crown and amide impregnated polymeric composites: PREC partitioning process, J. Chromatogr. A, 1157 (2007) 85–95.

[47] A. Zhang, Q. Hu, Z. Chai, SPEC: a new process for strontium and cesium partitioning utilizing two microporous silica-based supramolecular recognition agents impregnated polymeric composites, Sep. Sci. Technol., 44 (2009) 2146–2168.

[48] A. Zhang, C. Xiao, Q. Hu, Z. Chai, Synthesis of a novel microporous silica-calix[4]arene-crown supramolecular recognition material and its adsorption for cesium and some typical metals in highly active liquid waste, Solvent Extr. Ion Exch., 28 (2010) 526–542.

Supplementary information

Synthesis of bis-epoxides BE1 [1,2-bis(oxiran-2-ylmethoxy)benzene] and BE2 [2-(((2-(oxiran-2-ylmethoxy) phenyl) thio)methyl)oxirane].

BE1 and BE2 were synthesized according to a previously published procedure [S1,S2]. The procedures are described briefly.

BE1 was synthesized as follows: catechol (0.2 mol) was loaded in a 100 mL round bottom flask equipped with a magnetic stirrer. The flask was then attached to a reflux condenser fitted with a calcium chloride guard. Epichlorohydrin (0.86 mol) was added via α syringe. The mixture was stirred until all the catechol has dissolved. NaOH (0.8 mL, 10 N) was added via syringe, and the mixture was stirred for 48 h at 40°C under N_2 atmosphere. The mixture was cooled to room temperature, after which NaOH (842 mL, 5 N in saturated Na_2CO_3) was added. The mixture was stirred for another 20 h at room temperature under N_2 atmosphere. The crude product was collected in chloroform and then purified by silica gel chromatography (yield: 31.2 g, 69.72%).

Table S1
Recipe for the preparation of epoxy polymers using different bis-epoxides (BE*n*) and diamines at different bis-epoxide to solvent (BE*n*/DMSO) ratios

Entry	BE*n*, (mmol)	Diaminopropane, (mmol)	BE*n*/DMSO (wt/wt)	Product after curing
BE1-125-Pr	2.26	1.46	1.25	Solid (BE1-Ep-Pr)
BE1-83-Pr	2.26	1.45	0.83	Soft solid
BE1-63-Pr	2.26	1.45	0.63	Liquid
BE1-50-Pr	2.26	1.46	0.50	Liquid
Entry	BE*n*, (mmol)	Ethylenediamine, (mmol)	BE*n*/DMSO (wt/wt)	Product after curing
BE1-125-Et	2.27	1.51	1.25	Solid (BE1-Ep-Et)
BE1-83-Et	2.25	1.53	0.83	Soft solid
BE1-63-Et	2.28	1.50	0.63	Liquid
BE1-50-Et	2.27	1.54	0.50	Liquid
Entry	BE*n*, (mmol)	Diaminopropane, (mmol)	BE*n*/DMSO (wt/wt)	Product after curing
BE2-125	2.14	1.46	1.25	Solid, tough
BE2-83	2.14	1.47	0.83	Solid (BE2-Ep)
BE2-63	2.14	1.45	0.63	Solid, soft
BE2-50	2.14	1.46	0.5	Gel
BE3-125	1.96	1.33	1.25	Solid (BE3-Ep)
BE3-83	2.00	1.32	0.83	Soft solid
BE3-63	1.99	1.35	0.63	Soft solid
BE3-50	2.01	1.35	0.50	Soft solid

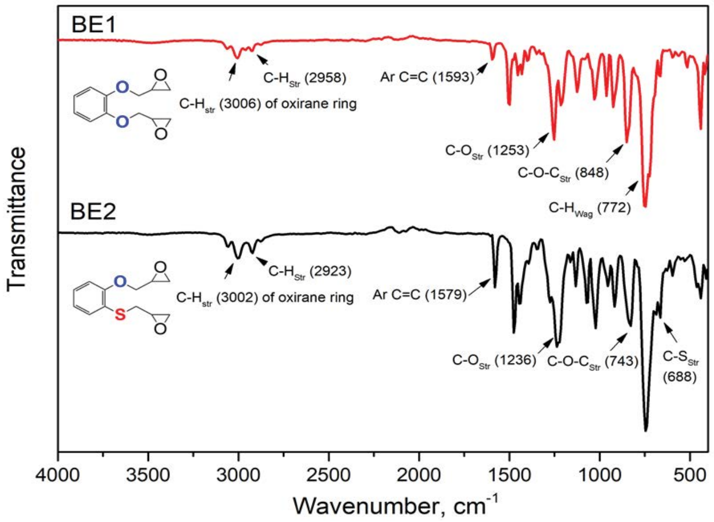

Fig. S1. FTIR spectra of bis-epoxides BE1 [1,2-bis(oxiran-2-ylmethoxy)benzene] and BE2 [2-(((2-(oxiran-2-ylmethoxy)phenyl)thio) methyl)oxirane].

BE2 was synthesized as follows: A 250 mL round bottom flask was loaded onto an ice bath and then attached to a reflux condenser. The reaction vessel was purged with N_2 for 15 min. Mercaptophenol (0.08 mol) and epichlorohydrin (0.32 mol) were added via syringe. NaOH (10 N, 0.4 mL) was added dropwise. The mixture was stirred for 48 h at 40°C under N_2 atmosphere and then cooled to room temperature. NaOH (60 mL, 5 N in saturated Na_2CO_3) was added. The mixture was stirred further for 24 h at room temperature under N_2 atmosphere. The crude product was collected in chloroform and then purified by silica gel chromatography (yield: 5.47 g, 26.99%).

The Fourier transform infrared spectroscopy (FTIR) spectra of BE1 and BE2 (Fig. S1) shows the signature peaks associated with their functional groups confirming their successful synthesis.

References

[S1] R.E.C. Torrejos, G.M. Nisola, H.S. Song, L.A. Limjuco, C.P. Lawagon, K.J. Parohinog, S. Koo, J.W. Han, W.-J. Chung, Design of lithium selective crown ethers: synthesis, extraction and theoretical binding studies, Chem. Eng. J., 326 (2017) 921–933.

[S2] R.E.C. Torrejos, G.M. Nisola, S.H. Min, J.W. Han, S. Koo, K.J. Parohinog, S. Lee, H. Kim, W.-J. Chung, Aqueous synthesis of 14–15 membered crown ethers with mixed O, N and S heteroatoms: experimental and theoretical binding studies with platinum-group metals, ChemPlusChem, 84 (2019) 210–221.